Distribution Category:
Magnetic Fusion Energy
(UC-20)

ANL/FPP/TM-203

ANL/FPP/TM--203

DE86 007263

ARGONNE NATIONAL LABORATORY
9700 South Cass Avenue
Argonne, Illinois 60439

NUCLEAR DATA NEEDS FOR FUSION REACTORS

by

Yousry Gohar

Fusion Power Program

Invited Paper Presented at the
International Conference on Nuclear Data for Basic and Applied Science
May 13-17, 1985, at Santa Fe, New Mexico

January 1986

LIST OF TABLES

TABLE OF CONTENTS

LIST OF FIGURES

NUCLEAR DATA NEEDS FOR FUSION REACTORS

By

Yousry Gohar

ABSTRACT

The nuclear design of fusion reactor components (e.g., first wall, blanket, shield, magnet, limiter, divertor, etc.) requires an accurate prediction of the radiation field, the radiation damage parameters, and the activation analysis. The fusion nucleonics for these tasks are reviewed with special attention to point out nuclear data needs and deficiencies which effect the design process. The main areas included in this review are tritium breeding analyses, nuclear heating calculations, radiation damage in reactor components, shield designs, and results of uncertainty analyses as applied to fusion reactor studies. Design choices and reactor parameters that impact the neutronics performance of the blanket are discussed with emphasis on the tritium breeding ratio. Nuclear data required for kerma factors, shielding analysis, and radiation damage are discussed. Improvements in the evaluated data libraries are described to overcome the existing problems.

1.0 INTRODUCTION

In order to address the subject of nuclear data needs for fusion reactors, it is essential to discuss some design issues which point out these needs and deficiencies in the current data libraries. In fusion reactors nucleonics, blanket and shield have three primary nucleonics goals: converting the kinetic energy of the fusion neutrons to sensible heat suitable for power generation, achieving a specific tritium breeding ratio, and reducing the neutrons and photons leakage intensities from the outer shield surfaces. In order to achieve these goals, an accurate prediction of the radiation field and nuclear responses in several reactor components are required. Three basic steps are included: a) evaluation of the radiation sources, b) transport of radiation from the source locations to the point of interest, and c) evaluation of the radiation effects in physical quantities to determine the operating conditions and the expected time to failure for each reactor component.

Fusion reactor design studies and fusion neutronics experiments require nuclear data in several areas like tritium breeding, nuclear heating, radiation damage, radiation shielding, activation, afterheat, etc. There have been several articles[1-11] discussing these different areas. An extensive report on the subject was given by Jarris[12] where various aspects of fusion neutronics were discussed. A recent compilation of the nuclear data needs for fusion energy was reviewed within the nuclear data base assessment for the International Tokamak Reactor (INTOR)[13].

This report reviews design issues and main reactor parameters which impact the neutronics performance of the different reactor components with emphasis on the nuclear data needs and deficiencies. The paper utilizes the most recent fusion studies rather than giving a historical review. The technical benefits and the better reactor economics of the D-T fuel cycle promote its use for the first generation of fusion reactors and this review. However, the D-D fuel cycle produces a 14-MeV neutron per each D-D reaction in the plasma assuming a complete burn for the tritium produced. So, the nuclear data required for the D-D fuel cycle are covered within the needs of the conventional D-T fuel cycle.

2.0 TRITIUM BREEDING REQUIREMENTS

The tritium breeding capability of the fusion blanket must be adequate to supply the tritium fuel requirement during the whole plant lifetime as well as generate enough surplus of tritium to start another reactor within a reasonable period of time. A 5-year period is considered adequate for fusion power based on the historical growth of the power industry. Several assessments[14-18] were carried out to study the tritium breeding requirements for fusion reactors. In general, the tritium breeding ratio required (T_r) for self-sufficiency can be expressed as

$$T_r = 1 + G$$

where G is the extra tritium produced per fusion neutron to insure self-sufficiency and produce the initial tritium inventory to start another reactor after operating the first reactor for a specific time (doubling time). This extra tritium production accounts for the losses and the radioactive decay of tritium from the whole system. T_r is a sensitive function of the doubling time and the reactor design parameters[14-18]. The main parameters include: a) the tritium inventories in the different reactor components, b) the tritium fractional burnup in the plasma, c) the tritium reserve to operate the reactor without the tritium recovery system, and d) the tritium losses and processing efficiencies. Figure 1 shows the relation between the tritium breeding ratio and the doubling time for different tritium inventories and a 0.4 tritium fractional burnup based on the STARFIRE design[19]. Figure 2 shows the required tritium breeding ratio as a function of the tritium fractional burnup at different values for the number of days of fuel reserve to operate the reactor without the tritium exhaust system calculated for the Blanket Comparison and Selection Study[18]. These calculations assume a 5-year doubling time and a 0.1% tritium processing efficiency. The results of Fig. 2 show that the required tritium breeding ratio is about 1.05 for 2 days of fuel reserve with a 0.1 tritium fractional burnup. Increasing the tritium fractional burnup reduces the required tritium breeding ratio as shown in Fig. 2 and improves the reactor performance[19,20]. For example, the fractional burnup values for STARFIRE and MARS are 0.42 and 0.14, respectively. The other important factor is the total tritium inventory which can burden the blanket design and the required tritium capability of the blanket.

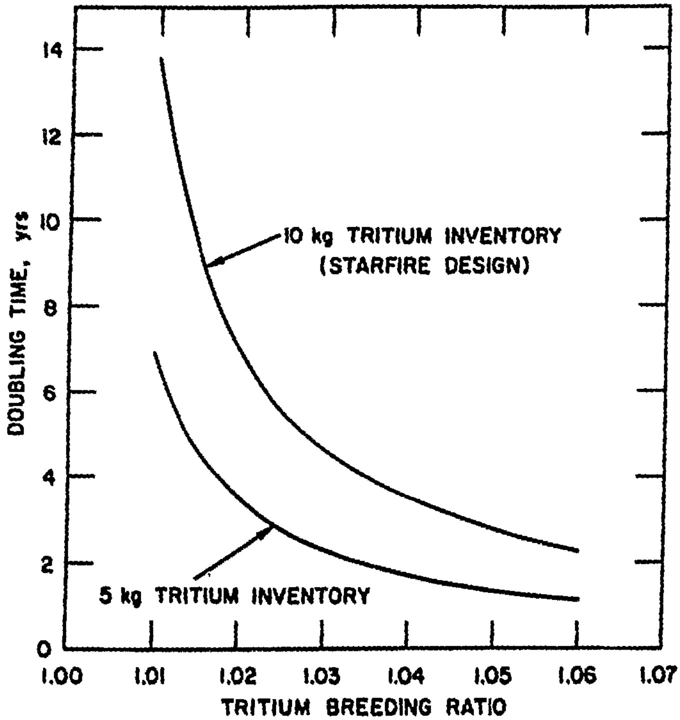

FIGURE 1. Doubling time as a function of tritium breeding ratio for STARFIRE design.

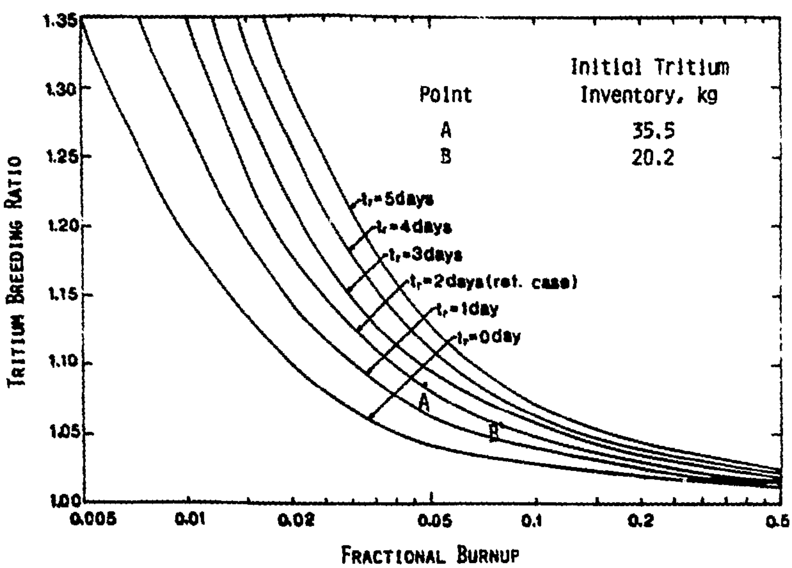

FIGURE 2. Required breeding ratio as a function of the tritium fractional burnup in the plasma at several values for the number of days of fuel reserve (t_r).

The Blanket Comparison and Selection Study[18] evaluated sixteen blanket concepts for electrical energy production. The tritium inventories calculated for these blanket concepts are shown in Table I. The liquid breeder blanket concepts have a low tritium inventory of less than 0.5 kg which reduces the required tritium breeding ratio. On the contary, the solid breeder blanket concepts have a larger tritium inventory with a maximum value of 2.4 kg. Also, there is a large uncertainty in the physical data related to the tritium recovery from the solid breeders which can increase the inventory by an order of magnitude[18]. For such a high inventory the required tritium breeding ratio is about 1.09 for the operating conditions discussed above.

Table I. *Tritium Inventories[a] and Tritium Breeding Ratios[b] for the* Sixteen Blanket Concepts of the Blanket Comparison and Selection Study[18]

Blanket Concepts[c]	Tritium Inventory (g)		Tritium Breeding	
	Tokamak	Mirror	Tokamak	Mirror
Li/Li/V	496	337	1.28	1.19
Li/Li/HT-9	-	340	-	1.14
Li/He/HT-9	349	237	1.16	1.17
17Li83Pb/17Li83Pb/V	-	1	-	1.18
Li_2O/He/HT-9	154	136	1.11	1.14
$LiAlO_2$/He/HT-9/Be	67	29	1.04	1.16
$LiAlO_2$/H_2O/HT-9/Be	2372	1557	1.16	1.22
$LiAlO_2$/NS/HT-9/Be	2109	304	1.24	1.29
Flibe/He/HT-9/Be	209	143	1.17	1.29

[a] Tritium reserve for operating without tritium exhaust system is not included.
[b] Values are based on three-dimensional analyses assuming STARFIRE and MARS geometrical models.
[c] The abbreviations are corresponding to breeder/coolant/ structure/neutron multiplier; Be-beryllium, NS-nitrate salt, $LiAlO_2$-γ lithium aluminate, HT-9 ferritic steel, Li-lithium, V-vanadium alloy, He-helium, Flibe-lithium beryllium fluoride salt.

3.0 TRITIUM BREEDING POTENTIAL OF DIFFERENT BLANKET CONCEPTS

Over the years, lithium and lithium compounds have been considered for tritium generation in fusion reactors. The liquid lithium itself has an upper limit of about 1.8 tritons per fusion neutron assuming an infinite medium[21]. Also, other lithium compounds or combination of materials (excluding fissionable materials) can produce up to 2.7 tritons per fusion neutron. However, several engineering considerations dictate the use of structure materials and coolant channels arranged in specific patterns to hold and cool the breeder materials. In all blanket concepts,[22-24] the calculated tritium breeding ratios are much lower than the upper theoretical limits of the breeder (or neutron multiplier - breeder combinations) materials. Table II gives the calculated tritium breeding ratios for the sixteen blanket concepts of the Blanket Comparison and Selection Study based on the geometrical models of STARFIRE and MARS[18,23]. The blanket concepts with liquid breeders have a higher tritium breeding potential relative to the other concepts. Neutron multipliers are incorporated with the solid breeders to enhance the tritium breeding potential and the blanket energy multiplications.

4.0 NEUTRON MULTIPLIER MATERIALS

Solid breeder blanket concepts have several important advantages in comparison with the other concepts. Unfortunately, the existence of the other elements in the lithium compounds and the high percentage of the structural material result in a tritium breeding ratio of less than one. The fusion neutron interactions with these elements reduce the tritium production from lithium-7. Furthermore, the parasitic neutron reaction in these elements results in less neutron capture in lithium-6 for tritium generation. Neutron mutliplier materials were introduced with solid breeder materials to get an adequate tritium breeding ratio. Examination of the nonfissionable elements with significant (n,2n) and (n,3n) cross sections and low neutron absorption indicates that Pb, Bi, Be and Zr have the highest potential for neutron multiplication[24]. Table II gives a list of the potential candidates along with some relevant parameters for each.

Table II. Properties of Candidate Neutron Multiplier Materials

Material	Be	BeO	Pb	PbO	Bi	Zr	Zr_5Pb_3	PbBi
Density, g/cm^3	1.85	2.96	11.34	9.53	9.8	7.6	8.93	10.46
Atoms or molecules/ cm^3, x 10^{-24}	0.124	0.0713	0.0335	0.0257	0.0282	0.0429	0.00468	0.0152
$\sigma(n,2n)$ at 14 MeV, barns	0.5	0.5	2.2	2.2	2.2	0.6	9.6	4.4
$\Sigma(n,2n)$ at 14 MeV, cm^{-1}	0.0618	0.0256	0.0737	0.0565	0.0621	0.0257	0.0449	0.0670
Threshold energy for (n,2n) cross section, MeV	1.868	1.868	6.765	6.765	7.442	7.274	6.765	6.765
$\sigma(n,\gamma)$ at 0.0253 eV, barns	0.0095	0.0095	0.17	0.17	0.034	0.18	1.41	0.204
$\Sigma(n,\gamma)$ at 0.0253 eV, cm^{-1}	0.00117	0.000671	0.00569	0.00437	0.000960	0.00772	0.00660	0.0031
Radioactivity isotopes	^{10}Be	^{10}Be	^{205}Pb	^{205}Pb	^{210}Po	^{93}Zr	^{93}Zr, ^{205}Pb	^{205}Pb, ^{210}Po
Decay types	B^-	B^-	Ec	Ec	α	B^-	B^-, Ec	Ec, α
Half lives	1.6×10^6 y	1.6×10^6 y	1.5×10^7 y	1.5×10^7 y	138.4 d	1.5×10^6 y	1.5×10^6 y 1.5×10^7 y	1.5×10^7 y 138.4 d
Melting point, °C	1278	2520	327.5	888	271.3	1852	1400	125
Thermal conductivity[a] at 25°C, W/m-°K	201	216[b]	35.3	2.8	7.92[c]	22.7	----	2.3[d]

[a] At 25°C.
[b] Pure beryllium oxide, hot pressed.
[c] Polycrystalline.
[d] At 200°C.

The performance parameters of the different neutron multipliers were compared through the use of a one-dimensional neutronics analysis for two different blanket concepts[24,25]. The key parameters are the tritium breeding ratio, the energy deposition per fusion neutron, and the long-term radioactivity from the multiplier material. In both blanket concepts $LiAlO_2$ solid breeder with 90% ^6Li enrichment, PCA steel structural material, and H_2O coolant are employed with different neutron multipliers. The neutron multiplier material is placed in a separate zone in front of the tritium breeding zone and behind the first wall. The differences between the two concepts are related to the neutron multiplier zone design. In the first concept the neutron multiplier is internally cooled by water tubes embedded inside the neutron multiplier material (internally cooled neutron multiplier) while the second concept uses the coolant in bounding walls (first and second) to remove the heat from the neutron multiplier material (externally cooled neutron multiplier). The volumetric compositions and dimensions of the multiplier zone are shown in Table III for both blanket concepts.

Table III. Blanket Parameters for Internally-cooled and Externally-cooled Neutron Multiplier Concepts

Zone Description	Zone Thickness cm	Zone Composition, Vol.%	
		Exter.-Cooled	Inter.-Cooled
First wall	1	50% PCA	50% PCA 50% H_2O50% H_2O
Neutron Multiplier	Variable	100% neutron multiplier	85% neutron multiplier 10% PCA 5% H_2O
Second wall[a]	1	25% PCA 25% H_2O	No second wall
Tritium breeder	50	80% $LiAlO_2$[b] 10% PCA 5% H_2O 5% He purge	80% $LiAlO_2$[b] 10% PCA 5% H_2O 5% He purge
Reflector	15	50% carbon 25% PCA 25% H_2O	50% carbon 25% PCA 25% H_2O

[a] Second wall is 50% by volume void.
[b] 90% ^6Li.

The tritium breeding ratio and the energy deposition per fusion neutron are plotted in Figs. 3 and 4, for the internally-cooled multiplier concept as a function of the neutron multiplier thickness, respectively. Beryllium and lead exhibit the highest tritium breeding ratios for this blanket concept. Beryllium produces the largest number of secondary neutrons compared to the other neutron multipliers; however, the maximum breeding ratio is about the same as for lead. This is primarily due to the softer spectrum from beryllium and the high slowing down power of the water coolant which increase the neutron losses in the structural material per fusion neutron. The unique feature of beryllium is the high energy deposition per fusion neutron which is very desirable from the economic point of view. Zr_5Pb_3 and PbO show a maximum tritium breeding ratio of 1.11 and 1.08, respectively, which is probably insufficient for a tokamak reactor. The tritium breeding capability from this blanket concept can be improved by using heavy water coolant[24,25] which has a lower slowing down power relative to the ordinary water.

In the second concept, the neutron multiplier is externally cooled from both sides which permits for a simpler mechanical design and improves the nuclear performance. The tritium breeding ratio and the energy deposition per fusion neutron are plotted in Figs. 5 and 6, respectively, as a function of the neutron multiplier zone thickness. Beryllium gives the highest tritium breeding ratio for this concept because the neutron slowing down by the water coolant and the parasitic reactions in the structural material of the neutron multiplier zone are eliminated. It is clear from Fig. 5 that the performance of the neutron multipliers are improved in the second blanket concept. Four neutron multiplier materials, Be, Pb, Zr_5Pb_3, and PbO provide a breeding ratio greater than 1.2. Bismuth is expected to match the lead performance since they are quite similar from the neutronics point of view. So, it appears that Be, Zr, Pb and Bi are the potential elements for neutron multiplication in fusion reactors. The physical characteristics of these elements limit their benefit to few blanket concepts. Bi and PbBi have low melting temperatures which restrict their use to the liquid phase for the power producing blanket. Also, the lead multiplier zone can be designed to match the operating temperature range for water-cooled blankets while it generates design problems for the helium-cooled blankets. Lead oxide was considered to overcome this temperature limit; it has a higher melting temperature. Its use as a neutron multiplier results in a lower tritium breeding ratio for the blanket than lead

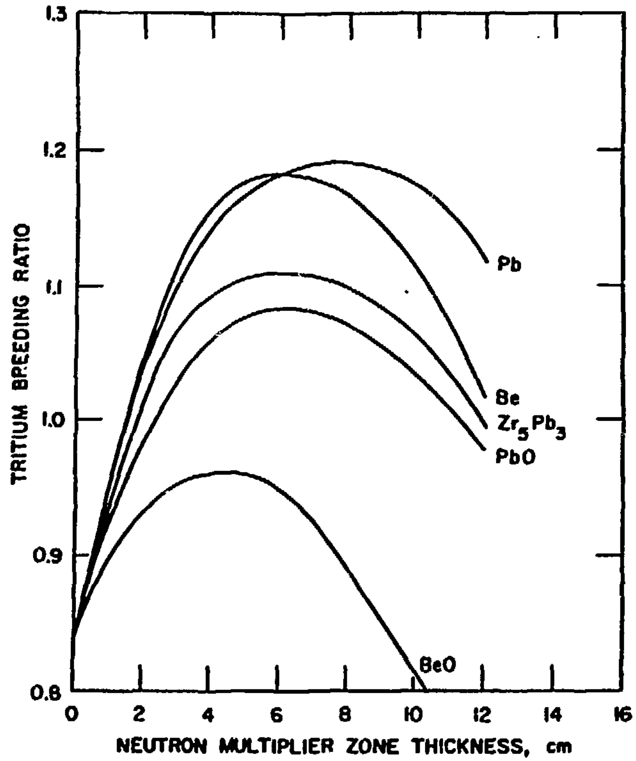

FIGURE 3. Tritium breeding ratio from $LiAlO_2$ (90% ^6Li) breeder/H_2O coolant/PCA steel structure blanket with different neutron multipliers (internally cooled).

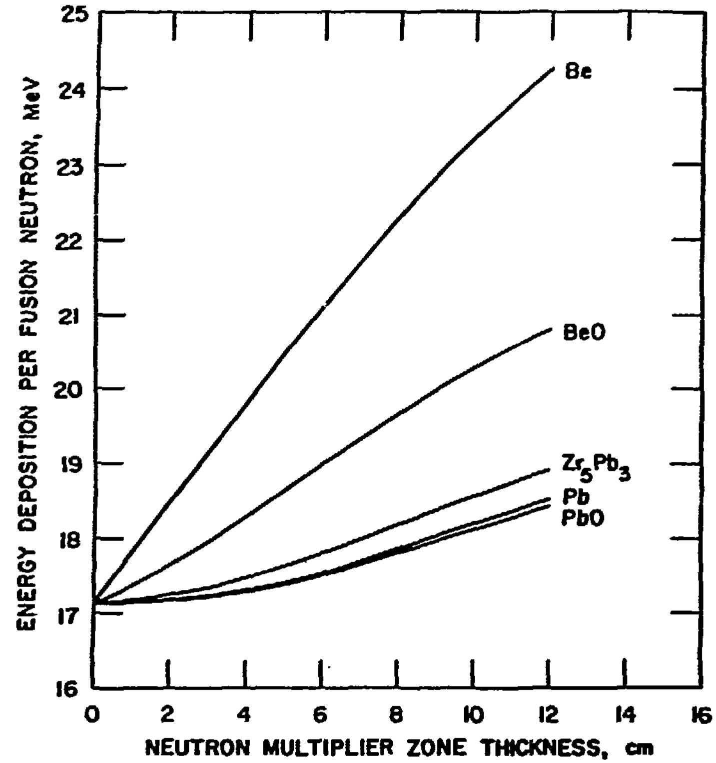

FIGURE 4. Energy deposition per fusion neutron from $LiAlO_2$ (90% ^6Li) breeder/H_2O coolant/PCA steel structure with different neutron multipliers (internally cooled).

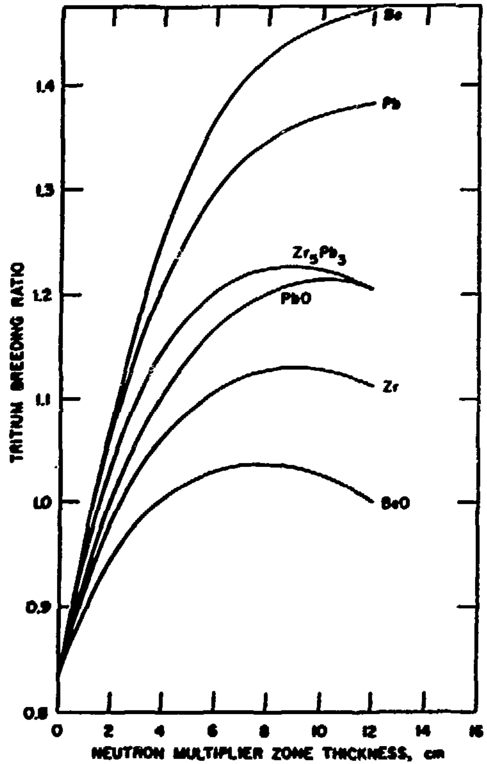

FIGURE 5. Tritium breeding ratio from $LiAlO_2$ (90% ^6Li) breeder/H_2O coolant/PCA steel structure blanket with different neutron multipliers (externally cooled).

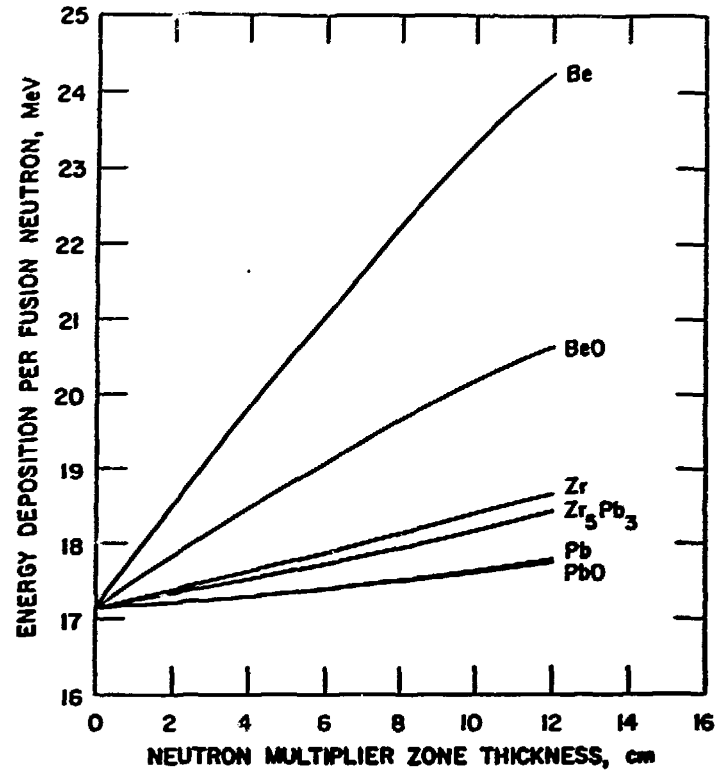

FIGURE 6. Energy deposition per fusion neutron from $LiAlO_2$ (90% ^6Li) breeder/H_2O coolant/PCA steel structure with different neutron multipliers (externally cooled).

due to the presence of oxygen atoms and lower lead density. Also, PbO has low thermal conductivity and an operating temperature limit of 540°C due to phase change which represents a challenge for the thermal hydraulic design. Beryllium neutron multiplier has a high temperature limit and produces more neutrons compared to other neutron multipliers. Beryllium has a resource limitation, toxicity problem, high swelling rate under irradiation, and a small tritium production rate. BeO eliminates some of the beryllium problems but it reduces the blanket neutronics performance.

The induced radioactivity in the neutron multipliers is small compared to the rest of the blanket. Beryllium has no long-term radioactivity, lead generates ^{205}Pb which decays by electron capture, and zirconium produces ^{93}Zr and ^{99}Nb isotopes. In general, it appears that Be, Pb, Zr_5Pb_3, BeO, and PbO are the most promising candidates.

5.0 AUXILIARY HEATING AND IMPURITY CONTROL

Fusion reactor designs incorporate several systems integrated in the blanket and shield for plasma operation which impact the reactor neutronic performance. Auxiliary heating and impurity control of the plasma have a significant impact on the tritium breeding ratio, the energy deposit in the blanket, and the shield volume. Radio-frequency and neutral beams are the primary techniques for auxiliary heating. For impurity control, limiters and divertors are under consideration.

Several studies were performed to quantify the impact of these systems on the reactor neutronics. In general, this impact increases with the decrease in the total cross section or the increase of the slowing down power of the blanket. Blankets are categorized fast or thermal based on the type of neutron interactions used for tritium breeding. Blankets are designated fast when a large fraction of the tritium is produced through $^7Li\ (n;n',\alpha)t$ reaction. On the contrary, thermal blankets depend mainly on $^6Li\ (n,\alpha)t$ reaction for tritium breeding. The relative reduction in the tritium breeding ratio due to the penetrations caused by these systems in the blanket is two to three times larger than the relative reduction in the first wall surface area covered by the breeder materials as the blanket classification changes from fast to thermal. Also, the poloidal location, the materials of these systems, and the spatial distribution of the DT neutrons effect the reduction in the tritium breeding ratio.

Meier[26] analyzed the effect of penetrations on the tritium breeding ratio for a DT point source located at the center of a spherical ICF reactor chamber. Figure 7 shows the relative reduction in the tritium breeding ratio as a function of the surface area used for beams for lithium and lithium-lead breeders. Seki, et al.[27] showed that the reduction in the tritium breeding ratio of the Fusion Experimental Reactor (FER) is 3.4% due to the neutral beam injectors.

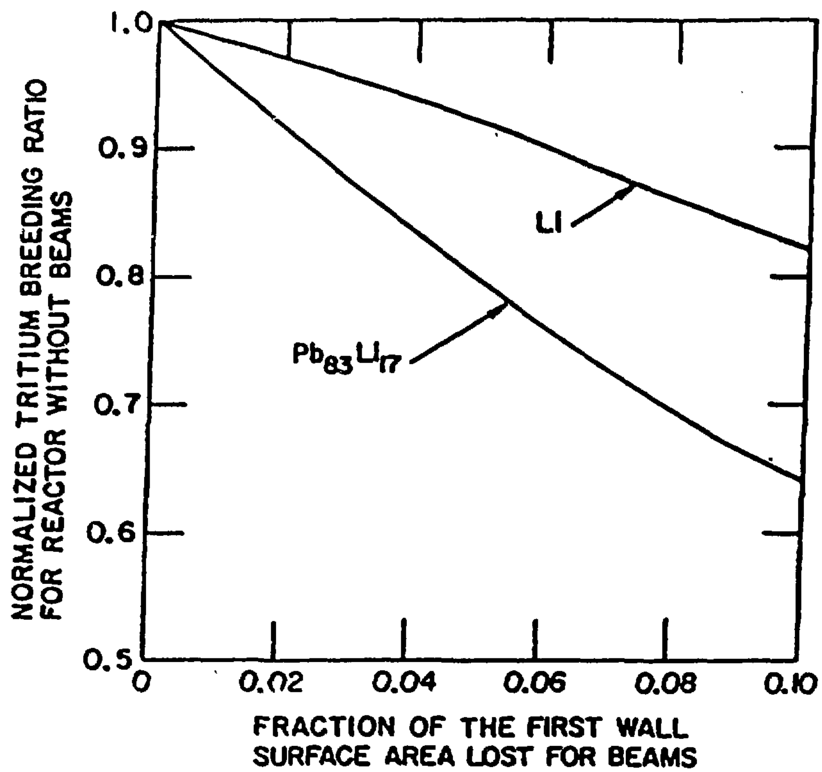

FIGURE 7. Tritium breeding ratio as a function of the fraction of the first wall surface area used for beam penetrations.

The limiter effect on the tritium breeding ratio was studied for several reactor designs[25,28,18]. The decrease in the tritium breeding ratio is 7.2% and 5.6% for the midplane and the bottom limiter for FED/INTOR reactor design with Li_2O breeder,[28] respectively. Recently, a detailed study[18] was performed to study the impact of several reactor design choices on the blanket neutronics performance including the impurity control system (limiter or divertor) and the material choice for the limiter. Figure 8 shows the geometrical models used in the analysis with lithium and lithium-lead breeders. The limiter-divertor comparison is displayed in Table IV. This study reached the following conclusions: a) Both limiter and divertor with liquid metal coolant (Li or 17Li83Pb) and vanadium structure have a negligible effect on the tritium breeding ratio, b) the limiter reduces the energy deposition in the blanket by about 3% relative to the divertor, and c) the limiter design with water coolant and copper structure material causes about 4% drop in the tritium breeding ratio relative to the lithium-vanadium limiter.

6.0 INBOARD BLANKET IN TOKAMAK REACTORS

Tokamak reactor designs call for reducing the thickness of the inboard section to improve performance and achieve better economics. This requirement dictates the use of an efficient shielding material to provide an adequate protection for the toroidal field coils and maintain small inboard thickness. Also, it is beneficial to avoid the use of tritium breeding blankets in this section because of their poor neutron attenuation characteristics. The elimination of the tritium breeding from the inboard section causes a serious drop in the tritium breeding ratio. This loss is a function of the blanket type (fast or thermal), the relative loss in the first wall area with tritium breeding materials, and the materials used for the nonbreeding section. For fast blankets, the relative drop in the tritium produced through $^7Li(n,n',\alpha)t$ is slightly greater than the relative loss in the first wall area with tritium breeding materials.[29,30] On the contrary, the relative drop in the tritium produced through $^6Li(n,\alpha)t$ is very sensitive to the materials used in the nonbreeding section[31,30,18] as well as the loss in the first wall with tritium breeding materials. Table V shows the impact of the inboard blanket design on the blanket performance for STARFIRE with different design choices. In this

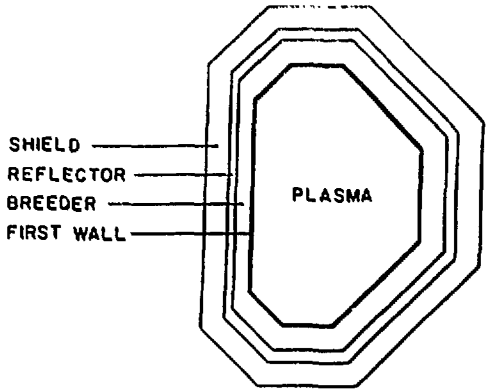

Reactor geometrical model with a tritium breeding blanket for the inboard and the outboard sections.

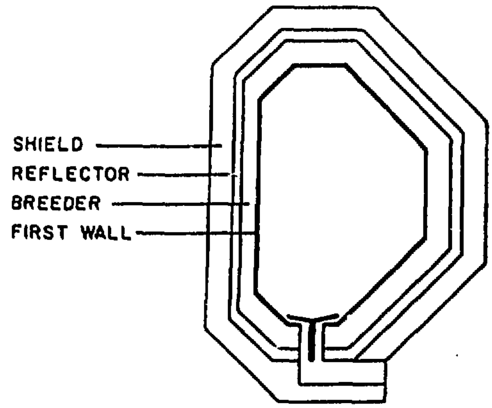

Reactor geometrical model with a tritium breeding blanket for the inboard and the outboard sections and a bottom limiter.

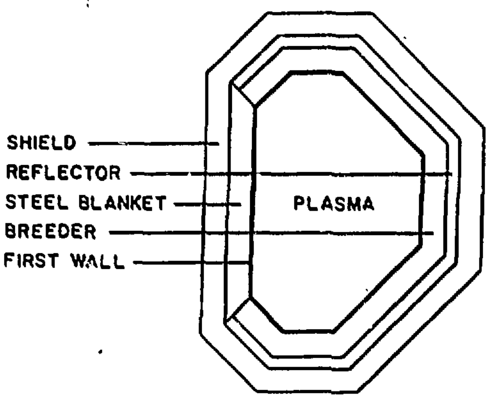

Reactor geometrical model with an outboard tritium breeding blanket, and an inboard steel blanket.

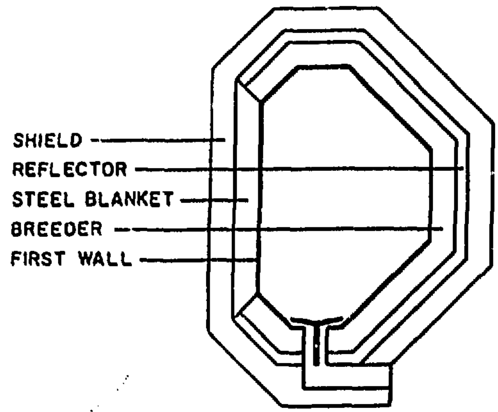

Reactor geometrical model with an outboard tritium breeding blanket, an inboard steel blanket, and a bottom limiter.

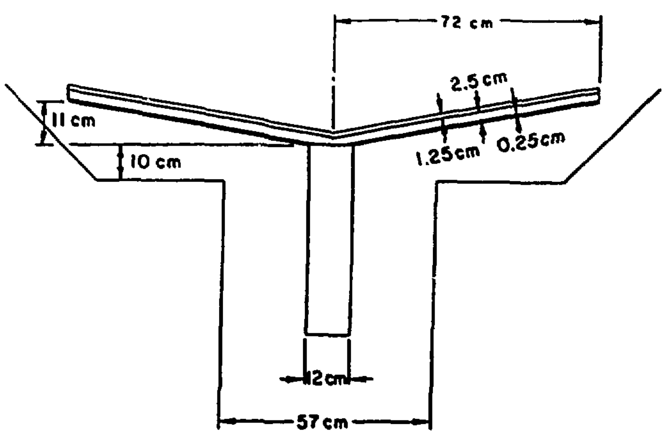

FIGURE 8. Geometrical model for the bottom limiter.

Table IV. Impact of the Impurity Control Option on the Blanket Performance in STARFIRE

A. Lithium Breeder

Inboard blanket materials	Li/PCA	Li/PCA	PCA/He	Li/PCA	PCA/He
Impurity control option	None	Divertor	Divertor	Limiter	Limiter
Divertor or limiter structural material	None	V15Cr5Ti	V15Cr5Ti	V15Cr5Ti	V15Cr5Ti
^{6}Li(n,α)T reaction rate per DTn	0.880	0.877	0.776	0.891	0.805
^{7}Li(n;n,′α)T reaction rate per DTn[a]	0.479	0.473	0.401	0.456	0.397
Tritium breeding ratio	1.359	1.350	1.177	1.347	1.202
Blanket energy deposition, MeV/DTn	18.78	18.56	18.93	18.23	18.34
Shield energy deposition, MeV/DTn	0.40	0.49	0.34	0.49	0.39

B. Lithium-Lead Breeder

Inboard blanket materials	17Li83Pb/PCA	17Li83Pb/PCA	PCA/He	17Li83Pb/PCA	PCA/He
Impurity control option	None	Divertor	Divertor	Limiter	Limiter
Divertor or limiter structural material	None	V15Cr5Ti	V15Cr5Ti	V15Cr5Ti	V15Cr5Ti
^{6}Li(n,α)T reaction rate per DTn	1.606	1.581	1.320	1.551	1.334
^{7}Li(n,n,′α)T reaction rate per DTn[a]	0.003	0.002	0.003	0.003	0.002
Tritium breeding ratio	1.609	1.584	1.317	1.554	1.336
Blanket energy deposition, MeV/DTn	17.07	17.13	17.80	16.53	17.07
Shield energy deposition, MeV/DTn	0.30	0.38	0.36	0.41	0.38

[a] Values are reduced by 15% to account for the change in the ^{7}Li cross sections.

Table V. Impact of the Inboard Blanket Design and the Limiter Option on the Blanket Performance in STARFIRE

	A. Lithium Breeder			
Inboard blanket materials	Li/PCA	Li/PCA	PCA/H_2O	PCA/He
Impurity control option	None	Cu-limiter	Cu-limiter	Cu-limiter
$^{6}Li(n,\alpha)T$ reaction rate per DTn	0.880	0.852	0.739	0.781
$^{7}Li(n;n,'\alpha)T$ reaction rate per DTn[a]	0.479	0.453	0.389	0.389
Tritium breeding ratio	1.359	1.305	1.123	1.170
Blanket energy deposition, MeV/DTn	18.78	18.02	18.53	18.26
Shield energy deposition, MeV/DTn	0.40	0.51	0.35	0.46
	B. Lithium-Lead Breeder			
Inboard blanket materials	17Li83Pb/PCA	17Li83Pb/PCA	PCA/H_2O	PCA/He
Impurity control option	None	Cu-limiter	Cu-limiter	Cu-limiter
$^{6}Li(n,\alpha)T$ reaction rate per DTn	1.606	1.522	1.228	1.294
$^{7}Li(n;n,'\alpha)T$ reaction rate per DTn[a]	0.003	0.003	0.002	0.002
Tritium breeding ratio	1.609	1.525	1.230	1.296
Blanket energy deposition, MeV/DTn	17.07	16.65	17.71	17.26
Shield energy deposition, MeV/DTn	0.30	0.43	0.29	0.41

[a] Values are reduced by 15% to account for the change in the ^{7}Li cross sections.

design, the inboard first wall is about 19% of the total first wall area. For the lithium-lead designs, the drop in the tritium breeding ratio is 20% and 15% for steel-water and steel-helium materials for the inboard blanket, respectively. The water coolant in the inboard blanket increases the neutron slowing down which increases (n,γ) reactions in the inboard blanket. This increase in the neutron absorption in the inboard blanket causes a 6% increase in the total energy produced in the blanket per fusion neutron as well as the drop in the tritium breeding ratio as shown in Table V. This effect is slightly moderated in the case of the lithium design. The use of carbon, beryllium, or lead in the nonbreeding section of the blanket reduces the impact of inboard blanket on the tritium breeding ratio. For the lithium oxide-He design in the STARFIRE reactor,[18] the decrease in the tritium breeding ratio is 8% and 2% for steel-He and lead-He, respectively.

6.1 Energy Multiplication

The main function of the blanket is to produce recoverable heat in suitable conditions for the thermal cycle. So, it is desirable to maximize the recoverable heat and just satisfy the other requirements, such as the tritium breeding. Three factors determine the blanket energy multiplication. These are the blanket materials (structure, breeder, coolant, and reflector), the total blanket thickness (first wall, breeding zone, and reflector zone), and the tritium breeding ratio required. The blanket energy multiplication is defined as the ratio of the energy deposited in the blanket from fusion neutron interactions and the fusion neutron energy.

Fusion neutrons suffer from the endothermic reactions in the slowing down process or the tritium production through the ^{7}Li (n;n,'α)t reaction. The ^{6}Li(n,α)t reaction and the radioactive capture in the blanket materials are exothermic reactions. However, the Q value for neutron capture in lithium-6 is only 4.78 MeV relative to more than 7 MeV for structure materials. This shows the motivation to design the blanket based on the minimum required tritium breeding ratio and capture the excess neutrons in the structure or the reflector materials. Figures 9 and 10 show the tritium breeding ratio and the blanket energy multiplication for self-cooled lithium-lead blankets as a function of the breeder zone thickness for different steel reflector zone thickness. For small reflector zone (less than 30 cm), the

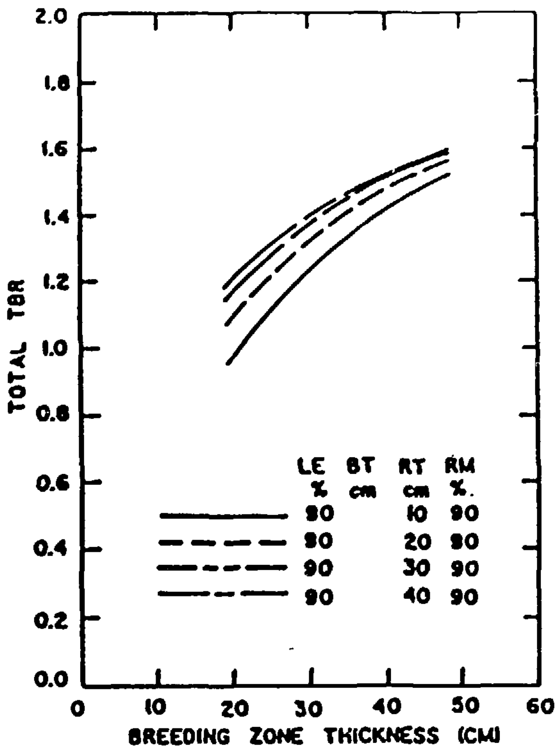

FIGURE 9. Tritium breeding ratio as a function of the lithium-lead breeding zone thickness for different steel reflector zone thicknesses with 90% lithium-6 enrichment.

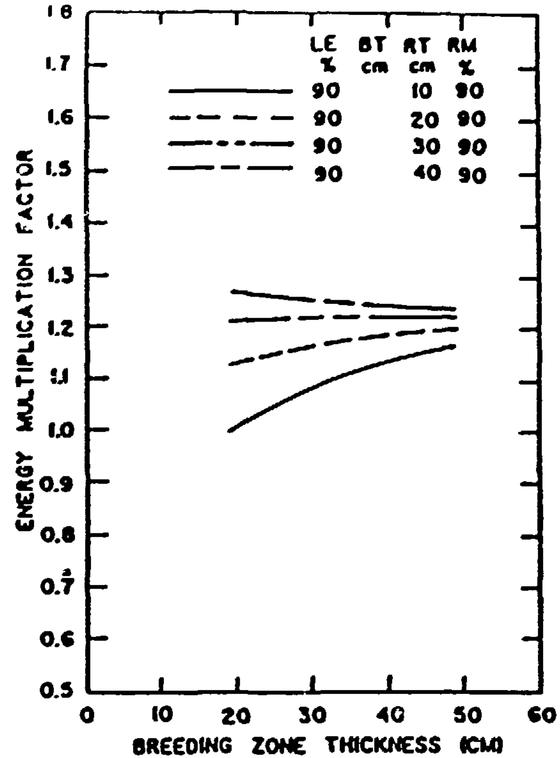

FIGURE 10. Blanket energy multiplication factor as a function of the lithium-lead zone thickness for different steel reflector zone thicknesses with 90% lithium-6 enrichment.

tritium breeding ratio and the energy multiplication saturate as the breeding zone thickness increases. However, for large reflector zone thickness, the increase in the tritium breeding ratio reduces the blanket energy multiplication because of the difference in the Q values explained before. A detailed study was conducted for lithium and lithium-lead breeders with steel and carbon reflector in reference 18. Sawan et al.[32,33] showed similar results for lithium and lithium-lead with water reflector as shown in Fig. 11 for self-cooled blanket concepts. Table VI shows the effect of the different reflector materials on the blanket energy. The choice of the reflector material is constrained by several considerations (activation, cost, weight, compatibility, etc.). Tungsten, steel, water, carbon, and lead are the primary candidates for the reflector zone.

Table VI. Impact of the Different Reflector Materials on the Lithium-lead Blanket[a] Performance

Reflector Material	Tritium Breeding Ratio	Blanket Energy Per DT Neutron
Mo	1.54	18.06
Cu	1.55	17.82
W	1.51	17.63
Type PCA Steel	1.59	17.36
H_2O	1.75	17.36
V15Cr5Ti Alloy	1.60	17.28
Zr	1.60	17.05
C	1.68	16.96
Pb	1.59	16.48
Al	1.57	16.47

[a] Blanket has a 1 cm first wall (50% 17Li83Pb, 50% type PCA steel), 49 cm breeding zone (95% 17Li83Pb, 5% type PCA steel), 30 cm reflector (5% 17Li83Pb, 90% reflector material, 5% type PCA steel), and 90% lithium-6 enrichment.

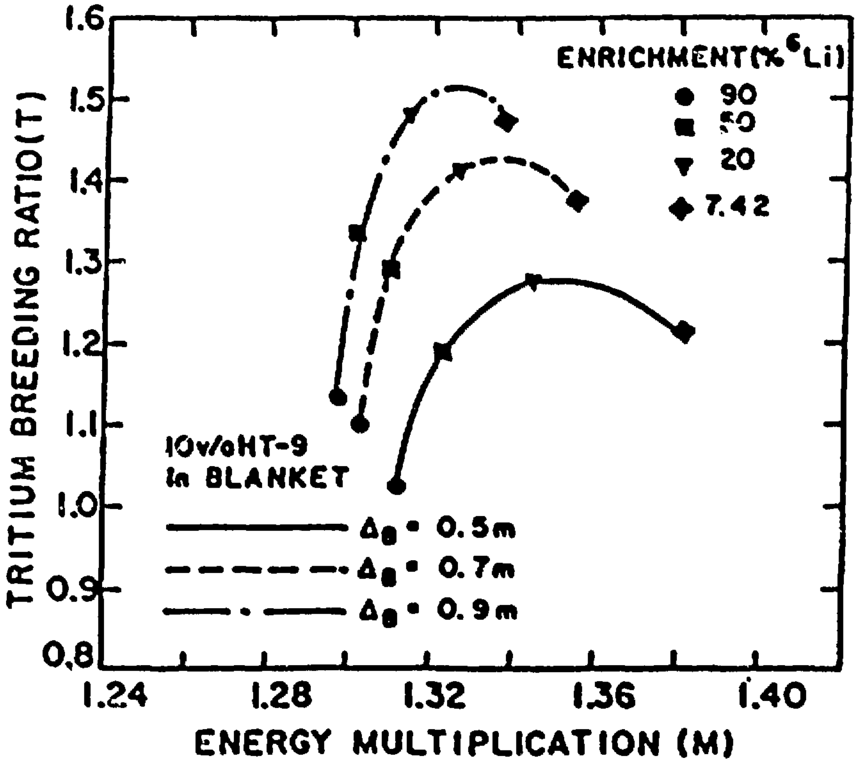

FIGURE 11. Tritium breeding ratio and blanket energy multiplication for different blanket thicknesses and lithium-6 enrichment.

7.0 RADIATION SHIELDING

The main function of radiation shielding in fusion reactors is to protect the different reactor components, the workers, and the general public from radiation effects. The most sensitive component is the magnets where they are required to function without change in their performance during the lifetime of the reactor. Therefore, the radiation shield must provide adequate protection for the different elements in the magnets from radiation damage and excessive nuclear heating.

For superconductor materials, fast neutron ($E > 0.1$ MeV) irradiation reduces the critical current density (J_c) and the critical temperature (T_c). For NbTi superconductor, it has been shown that J_c is decreased by about 10% at 4×10^{18} n/cm^2 fast fluence while T_c is unchanged[34,35]. Irradiation experiments at RTNS-II on NbTi superconductor[36] show consistency with previous results. At higher neutron fluence, the critical current degradation is expected to saturate[37], however experimental verification at 4°K is lacking. On the other hand, J_c of Nb_3Sn generally increases, reaching a maximum, and then decreases as the neutron fluence increases[38]. Irradiation experiments[35,36] at 6°K with 4×10^{18} n/cm^2 fast neutron fluence show that the maximum value and the increased rate of J_c increase with magnetic field. At a magnetic field of 5 T, the 6°K experiment resulted in a 16% increase in J_c at 2×10^{18} n/cm^2 without reaching a peak. At higher temperatures (350°K), irradiation experiments show the same behavior for J_c. However, the J_c peak was lower than the corresponding value at lower temperature for the same magnetic field. For example, the 350°K irradiation gave an 8% increase corresponding to the 16% obtained at 6°K. Other experiments[39] at 400°K with 10 T field resulted in a 90% increase for J_c at 4.4×10^{18} n/cm^2 and dropped to the original value at 10^{19} n/cm^2. Based on these experimental results,[34,38,40] the comparison between the room temperature, and the 6°K irradiation results; a fast neutron fluence above 10^{19} n/cm^2 can be used with Nb_3Sn without a decrease in the critical current density.

The stabilizer materials (Cu or Al) carry the magnet current in the event that the superconductor temporarily becomes resistive. The magnet is designed to remove the generated heat (I^2R) so that the normal region does not propagate. The stabilizer resistance is the most important parameter for this process. The total resistivity, ρ, of the copper stabilizer can be described as the sum of three components: the initial resistivity, ρ_o, the magnetoresistivity, ρ_μ, the irradiation induced resistivity, ρ_{irr}. Magnetoresistance is a function of ρ_o, ρ_{irr}, and the magnetic field which complicates the evaluation of ρ. Few experimental studies[36,41-45] have been done on the change of copper resistivity as a function of magnetic field, neutron fluence ($E > 0.1$ MeV), and a number of cycles of alternate neutron irradiation at 4°K and annealing at 300°K. The change in the copper resistivity in the magnet design can be accommodated by using more copper stabilizer which increases the thickness of magnet, can be partially annealed out by warming the coils, can be reduced by improving the shielding performance, or design the magnet at the saturation resistivity of the stabilizer material.

The most sensitive component in the magnets is the insulator materials. They suffer from irreversible damage which limits the operating life of the magnets in the power reactor designs[18-20]. The properties of interest for the coil designs are the electrical resistivity, dielectric strength, mechanical strength, and thermal insulation. Experimental results[45-48] from neutron irradiation at 5°K suggests that pclyimides can withstand a radiation dose of 10^{10} rads and retain high resistivity and mechanical strength. Glass cloth reinforced epoxy type G10-CR or G11-CR shows a serious degradation at 2 x 10^9 rads. The current designs assume a 10^{10} rads maximum tolerable dose in the insulator materials at the end of life.

The nuclear heating in the magnets impacts the refrigeration power required for the operation and represents the main design criterion for next generation devices with low neutron fluence.[49-55] At 4°K, about 500-watts of electrical power is consumed to remove one watt of nuclear heating. This low removal efficiency calls for minimizing the nuclear energy deposited in the magnets.

The personnel access to the reactor hall after a cooling period requires the satisfaction of regulation pertaining to occupational exposure. The regulations[56,57] limit the occupational dose to 5 rem/y with a maximum of 3 rem/quarter. Occupational exposure based on working 8 h per day and 40 h per week is 2.5 mrem/h. However, the current practice in the nuclear industry and the exposure policy of the U.S. Department of Energy are to reduce radiation exposures as low as reasonably achievable (ALARA). Specifically, for facilities being designed, an exposure level less than one-fifth of the maximum permissible dose equivalent should be used as a design objective.

Trade-off studies and optimization analyses were performed to define shielding materials, compositions, and thicknesses based on design requirements, performance, and cost. The nuclear responses in the magnets, the dose equivalent after shutdown in the reactor hall, and the induced radioactivity are the indicators for the shield performance. Several shielding options (steel/H_2O/B_4C/Pb, W/H_2O/B_4C/Pb, W/TiH_2/H_2O/B_4C/Pb, steel/H_2O/B_4C/Pb/H_2O/B_4C/Pb, and steel/H_2O/B_4C/Pb/concrete B_4C/Pb) were analyzed.[19,20,49/55,58-60]

8.0 CROSS SECTION UNCERTAINTY ANALYSIS

In fusion reactor conceptual designs, optimization studies are usually performed to achieve the best possible performance and satisfy the design requirements. For example, the neutronics aspects of the design require a specific tritium breeding ratio, maximum blanket energy multiplication, minimum blanket and shield thickness, and minimum energy deposition in the shield. Achieving the specified tritium breeding ratio is crucial for the viability of the design which focuses the attention on the uncertainty in the neutronics calculations. Especially, adding a margin in the required nuclear responses leads to an increase in the capital cost and reduces the performance. The relation between the tritium breeding ratio and the blanket energy multiplication discussed before gives an example of the negative impact on the reactor performance when a tritium breeding margin is considered. In this section, only the uncertainty resulting in the tritium breeding ratio due to uncertainties in the basic nuclear data in ENDF/B-V are discussed.

Neutron cross section sensitivity and uncertainty methods as applied to fusion neutronics were recently reviewed by several authors[12,61-63]. Historically, sensitivity analysis was performed to study the changes in the nuclear responses per unit change in a specific cross section. The results of these analyses are utilized in two different ways: a) identify the nuclear data needs for fusion reactors, and b) define the uncertainty in the nuclear responses when incorporated with the cross-section uncertainty. However, such results should be considered with caution because they are design dependent.

Recently, Youssef[61] presented estimates for the uncertainty in the tritium breeding due to uncertainties in the nuclear data based on one-dimensional calculations for four different blankets as shown in Table VII. The uncertainty in the tritium breeding ratio is in the range of 2 to 5% for the blanket concept considered. These values are relatively small if it is compared to the other design uncertainties discussed before.

Table VII. Uncertainty in the Tritium Breeding Ratio Due to the Cross Section Uncertainties

Blanket Concept Breeder/coolant/structure/neutron multiplier	Uncertainty in Tritium Breeding Ratio
17Li-83Pb/17Li-83Pb/PCA	± 3.95%
Li_2O/He/PCA	± 4.92%
$LiAlO_2$/H_2O/HT-9/Be	± 2.10%
Flibe/He/HT-9/Be	± 3.41%

9.0 NUCLEAR DATA NEEDS

Fusion reactors require a large range of nuclear data including cross sections for neutron and photon transport, nuclear response functions (kerma factors, atomic displacement data, gas production cross-sections, etc.) for design analyses, and covariances for uncertainty calculations. These data are generated from the evaluated data libraries such as ENDF/B[64], ENDL[65], JENDL[66], and UKNDL[67]. These libraries are created by combining the available experimental data and nuclear model code calculations. Most of the fusion materials shown in Table VIII are lacking experimental data above 6-MeV[11] where nuclear model codes are used to supply data for this energy range. The nuclear cross section theories and the nuclear model codes have been developed to provide more reliable data. These developments were reviewed by Dudziak[68], Gardner[69], and Young[70]. Over the last decade, the nuclear data program has focused on the measurement of differential nuclear data to satisfy high priority nuclear data needs of the fusion program[10]. Also, improved nuclear model code calculations and gamma-ray production data have been included in the evaluated

Table VIII. Candidate Fusion Materials

Tritium breeders:	Li, 17Li83Pb, Li-Pb-Bi, Li_7Pb_2, Li_2O, $LiAlO_2$, Li_2SiO_3, Li_8ZrO_6, Flibe
Structure: base	Austenitic stainless steel, ferritic steels, nickel-alloys, vanadium alloys
Coolant:	Li, 17Li83Pb, H_2O, D_2O, He, nitrate salt
Neutron multiplier:	Be, BeO, Pb, PbO, Bi, PbBi, Zr, Zr_5Pb_3
Limiter/divertor:	Cu, W, Ta, V alloys (structure); Water, Li, LiPb (coolant)
Wall protection:	Be, SiC, TiC, C
Hybrids:	U, Th (fuel cycles)
Shield:	Stainless steel, ferritic steel, tungsten, water TiH_2, concrete, B_4C, Pb
Magnet:	Cu, Al (stabilizer); NbTi, Nb_3Sn (superconductor); $MgAl_2O_4$, MgO, Y_2O_3, hydrocarbons (insulators)

Table IX. $^7Li(n;n',T)\alpha$ Recent Measurements and Evaluations

Value	Reference
Measurements	
0.302 ± 0.015b ($\bar{E}_n$ = 14.94 ± 0.05 MeV)	72
0.301 ± 0.016b ($\bar{E}_n$ = 14.74 ± 0.02 MeV)	73
0.235 ± 0.011b (E_n = 14.1)	74
0.242 ± 0.011b (E_n = 14.1)	74
0.256 ± 0.016b (E_n = 15.03)	75
Evaluations	
0.286b (E_n = 14 MeV)	76
0.289b (E_n = 15 MeV)	77
0.301b (E_n = 15 MeV)	65

data libraries. Lithium-7 gives an example of data improvements where accurate measurements and careful evaluations were performed by several groups[71-77,65]. Table IX gives the new values for the $^7Li(n;n',T)\alpha$ cross section around 14 MeV. However, several improvements in the evaluated data libraries are badly needed to overcome the known deficiencies. In the rest of this section, the main deficiencies will be highlighted and specific data needs will be pointed out.

The energy balance of the evaluated nuclear data libraries is the most important issue which has a serious impact on the fusion reactor designs. Nuclear heating profiles in the different reactor components, blanket energy multiplication factors, and shield requirements for coil protection are calculated through the use of kerma (the kinetic energy releases in a material) factors which are very sensitive to this issue. The kerma factor for a neutron with energy E can be written[78] as

$$K(E) = \sigma_t \left(E + \Sigma_i \frac{\sigma_i}{\sigma_t} Q_i + \Sigma_i \frac{\sigma_i}{\sigma_t} \overline{E}_{di} - \Sigma_j \frac{\sigma_j}{\sigma_t} \overline{E}_{n'j} - \Sigma_g \frac{\sigma_g}{\sigma_t} \overline{E}_{Gg}\right)$$

where σ_t is the total cross section and the terms in parenthesis are the fractioanl energy contributions from the individual reactions weighted by the probability of their occurrence. The first term is the energy brought into the reaction, Q is the reaction energy defined by mass conservation, $\overline{E}_d$ is the average decay energy, $\overline{E}_{n'}$ is the average secondary neutron energy, and E_G is the average photon energy. Based on the above equation, ENDF/B can be used to calculate the neutron kerma factors assuming the existence of the gamma production data. Negative kerma factors may result if the energy of the secondary neutrons or photons is overestimated. Obviously, the reverse situation is possible and it is more difficult to point out. Also, the same problem occurs for the element with several isotopes when natural evaluation is only given. In fact, ENDF/B-V processing[79,80] reveals that most of the fusion elements listed in Table VIII are suffering from negative kerma factors. However, the new evaluations for iron[81] and tungsten[82] are significantly improved with respect to this problem since the energy balance had been considered in the evaluation process[83]. So it is strongly recommended that future libraries consider the energy balance in the evaluation process and isotopic evaluations for the elements with several natural isotopes.

The other approach for calculating the neutron kerma factors depends only on the neutron data files in ENDF/B and the reaction kinematics. This approach provides an accurate recoil energy for scattering and radioactive capture. For other reaction types, several approximations are required to substitute for the missing data[78,83,84]. However, future ENDF/B versions are expected to include distributions for the products in energy and angle for each reaction which eliminates the need for these approximations[84]. This solution helps the neutron kerma calculations but the energy balance problem requires adjustment for the gamma production data to calculate correctly the photon energy deposited in the reactor.

The radiation damage calculations require detailed information about the reaction products. The current ENDF/B-V format does not permit the inclusion of such information which motivates the introduction of file-6 for future ENDF/B versions. MacFarlane and Foster[84] demonstrated the importance of including such data in the radiation damage calculations.

Fusion-fission hybrid reactors require the cross-sections for ^{238}U, ^{237}Th, and the other isotopes leading to the production of fissile materials. The (n,2n) and (n,3n) reactions are important for fissile production where new measurements were completed at Los Alamos National Laboratory.[10] Jarvis[12] listed the isotopes involved in the different fuel cycles and will not be repeated. Covariance data were included in ENDF/B-V for the smooth cross sections. However, covariances for angular distributions or secondary energy distributions are missing. Such data are required for the evaluation and the comparison of different design concepts.

REFERENCES

1. C. R. Head, Nuclear Data Requirements of the Magnetic Fusion Power Program of the United States of America, Proceedings of the Advisory Group Meeting on Nuclear Data for Fusion Reactor Technology, IAEA-TECDOC-223, p. 1, IAEA, Vienna (1979).

2. G. Constantine, Nuclear Data Requirements for Fusion Reactor Design-Neutronics Design, Blanket Neutronics and Tritium Breeding, ibid, p. 11.

3. Y. Seki, Review of Nuclear Heating in Fusion Reactors, ibid, p. 31.

4. O. N. Jarvis, Nuclear Data Requirements for Transmutation and Activation of Reactor Wall and Structural Materials, ibid, p. 47.

5. S. M. Qaim, Nuclear Data Needs for Radiation Damage Studies Relevant to Fusion Reactor Technology, ibid, p. 75.

6. M. A. Abdou, Nuclear Data Requirements for Fusion Reactor Shielding, ibid, p. 91.

7. D. V. Narkovskii and G. E. Shatalov, Neutron Data for Hybrid Reactor Calculations, ibid, p. 111.

8. M. R. Bhat and M. A. Abdou, Nuclear Data Requirements for Fusion Reactor Nucleonics, Proceedings of the Fourth Topical Meeting on the Technology of Controlled Nuclear Fusion Energy, CONF-801011, Volume 1, p. 405, King of Prussia, Pennsylvania (1981).

9. D. J. Dudziak and P. G. Young, Review of New Developments in Fusion Reactor Nucleonics, ibid, p. 419.

10. R. C. Haight, D. C. Larson, and Panel Members, Office of Basic Energy Sciences Program to Meet High Priority Nuclear Data Needs of the Office of Fusion Energy - 1983 Review, UCID-19930, Lawrence Livermore National Laboratory (Oct. 1983).

11. E. T. Cheng, Nuclear Data Needs for Fusion Energy Development, Proceedings of the Sixth Topical Meeting on the Technology of Controlled Nuclear Fusion Energy, San Francisco, CA (1985).

12. O. N. Jarvis, Nuclear Data for Fusion Reactors, European Applied Research Report - Nucl. Sci. Tech., Volume 3, Number 1/2, p. 127 (1981).

13. Y. Gohar, et al., Nuclear Data Base Assessment - Group H, USA Contribution to the International Tokamak Reactor - Chapter X - Section 2, October, 1984.

14. W. F. Vogelsang, Breeding Ratio, Inventory, and Doubling Time in a D-T Fusion Reactor, J. of Nucl. Tech. 15, 470 (1972).

15. D. Okrent, et al., On the Safety of Tokamak-Type, Central Station Fusion Power Reactors, Nucl. Eng. Design 39, 215 (1976).

16. M. A. Abdou, Tritium Breeding in Fusion Reactors, Proceedings of the International Conf. on Nucl. Data for Sci. and Tech., Sept. 6-10, 1982, p. 293, Antwerp, Belgium (1983).

17. J. Jung, An Assessment of Tritium Breeding Requirements for Fusion Power Reactors, ANL/FPP/TM-172, Argonne National Laboratory (1983).

18. D. L. Smith, et al., Blanket Comparison and Selection Study - Final Report, ANL/FPP-84-1, Argonne National Laboratory (1984).

19. C. C. Baker, et al., STARFIRE - A Commercial Tokamak Fusion Power Plant Study, ANL/FPP-80-1, Argonne National Laboratory (1980).

20. B. G. Logan, et al., MARS: Mirror Advanced Reactor Study Final Report, UCRL-53980, Lawrence Livermore National Laboratory (1984).

21. R. W. Moir, The Fusion-Fission Fuel Factory, Chapter 15 in Fusion, Edward Teller, Ed., Vol. 1, Part B, Academic Press, Inc.

22. M. A. Abdou, et al., Blanket Comparison and Selection Study Interim Report, ANL/FPP-83-1, Argonne National Laboratory (1983).

23. J. Jung and J. V. Foley, A Comparative Multidimensional Nuclear Analysis of Candidate Blanket Designs for Tokamak and Tandem Mirror Reactor Concepts, to be published (1985).

24. Y. Gohar, An Assessment of Neutron Multiplier for DT Solid Breeder Fusion Reactors, Transaction of American Nuclear Society 34, 51 (1980).

25. Y. Gohar and M. A. Abdou, Neutronic Optimization of Solid Breeder Blankets for STARFIRE Design, Proceedings of the Fourth Topical Meeting on the Technology of Controlled Nuclear Fusion Energy, Conf-801011, Volume II P.628, King of Prussia, Pennsylvania (1981).

26. W. R. Meier, Neutron Leakage Through Fusion Chamber Ports: A Comparison of Lithium and Lithium-Lead Blankets, J. of Nucl. Tech. 3, 385 (1983).

27. Y. Seki, et al., Neutronics Design of FER Blanket/Shield, US-Japan Workshop on Blanket Design/Technology held at Argonne National Laboratory on Nov. 10-11, 1982.

28. Y. Gohar, Limiter Impact on the Tritium Breeding Ratio in a FED/INTOR Reactor, Transaction of American Nuclear Society 44, 140 (1983).

29. W. M. Stacey, Jr., et al., U.S. INTOR, the U.S Contribution to the International Tokamak Reactor Phase-1 Workshop - Assessment of a Tritium Breeding Blanket for INTOR INTOR/NUC/80-9, June 1980.

30. W. R. Meier, SEBREZ: An Inertial Fusion Reactor Concept, Trans. of Am. Nucl. Soc. 39, 246 (1981).

31. Y. Gohar, et al., Neutronic and Photonic Analysis of UWMAK-III Blanket and Shield in Noncircular Toroidal Geometry, Proceedings of the Second Topical Mtg. on the Technology of Controlled Nuclear Fusion, Conf-760935, Volume III, p. 833, Richland, WA (1976).

32. M. E. Sawan and J. H. Huang, The Tritium Breeding Energy Multiplication (T-M) Plot for Fusion Blanket Design, Trans. Am. Nucl. Soc., 44, 146 (1983).

33. M. E. Sawan and J. H. Huang, The Tritium Breeding-Energy Multiplication (T-M) Plots for Self Cooled Lithium Blankets, Trans. Am. Nucl. Soc., 46, 231 (1984).

34. B. S. Brown, Radiation Effects in Superconducting Fusion Magnet Materials, J. of Nucl. Mater. 97, 1 (1981).

35. M. Soell, Influence of Radiation Damage on the Maximum Attainable Magnetic Field for Toroidal Fusion Magnet Systems, J. of Nucl. Mater. 72, 168 (1978).

36. R. A. Vankonynenburg, et al., Fusion Neutron Damage in Superconductors and Magnet Stabilizers, J. of Nucl. Mater. 103&104, 18 (1979).

37. C. L. Snead, Jr. and T. Luhman, Radiation Damage and Stress Effects in Superconductors: Materials for High-Field Applications, BNL(33230), Brookhaven National Laboratory Report

38. B. S. Brown and T. H. Blewitt, Critical Current Density Changes in Irradiated Nb_3Sn, J. of Nucl. Mater. 103&104, 18 (1979).

39. A Tandem Mirror Technology Demonstration Facility, Lawrence Livermore National Laboratory, UCID-19328 (1983).

40. C. L. Snead, Jr., et al., High-energy-neutron Damage in Nb_3Sn: Changes in Critical Properties, and Damage-energy Analysis, J. of Nucl. Mater. 103&104, 749 (1981).

41. C. E. Klaburde, et al., The Effects of Irradiation on the Normal Metal of Composite Superconductor: A Comparison of Copper and Aluminum, J. of Nucl. Mater. 85&86, 185 (1979).

42. J. M. Williams, et al., The Effects of Irradiation on the Copper Normal Metal of a Composite Superconductor, IEEE Trans. on Magnetics 15, 731 (1979).

43. S. Tokamura and T. Kato, The Effects of Low Temperature Irradiation and Other Materials for Superconducting Magnets, J. of Nucl. Mater. 103&104, 729 (1981).

44. M. W. Guinan, Radiation Effects Limits on Copper in Superconducting Magnets, Lawrence Livermore National Laboratory, UCID-19800 (1983).

45. R. R. Coltman, Jr., Organic Insulators and the Copper Stabilizer for Fusion Reactor Magnets, Intl. Conf. on Neutron Irradiation Effects, Nov. 9-12, 1981, Argonne National Laboratory, Argonne, IL.

46. R. R. Coltman, Jr., et al., Radiation Effects on Organic Insulators for Superconducting Magnets, ORNL/TM-7077, Oak Ridge National Laboratory (1979).

47. R. H. Kernohan, et al., Radiation Effects on Organic Insulators for Superconducting Magnets, ORNL/TM-6708, Oak Ridge National Laboratory (1978).

48. F. W. Clinard, Jr., and G. F. Hurley, Ceramic and Organic Insulators for Fusion Applications, J. of Nucl. Mater. 103&104, 705 (1981).

49. Y. Gohar, Neutronics Activities for Next Generation Devices, Proc. of the 6th Topical Mtg. on the Tech. of Fusion Energy, San Francisco, CA, March 3-7, 1985.

50. S. Yang and Y. Gohar, TFCX Shielding Optimization, Proc. of the 6th Topical Mtg. on the Tech. of Fusion Energy, San Francisco, CA, March 3-7, 1985.

51. V. D. Lee and Y. Gohar, Shield Design for Next-Generation Low Neutron Fluence Superconducting Tokamaks, Proc. of the 6th Topical Mtg. on the Tech. of Fusion Energy, San Francisco, CA, March 3-7, 1985.

52. C. A. Flanagan, Tokamak Fusion Core Experiment: Design Studies Based on Superconducting and Hybrid Toroidal Field Coils, Design Overview, ORNL/FEDC-84/3, Oak Ridge National Laboratory (1984).

53. Y. Gohar and M. A. Abdou, U.S. INTOR Radiation Shield Design, Proc. of the 6th Intl. Conf. on Radiation Shielding, Tokyo, Japan (1983).

54. Y. Gohar and M. A. Abdou, INTOR Radiation Shielding for Personnel Access, Ninth Symp. on Engineering Problems of Fusion Research, Chicago, IL (1981).

55. C. A. Flanagan, et al., Fusion Engieering Device Design Description, ORNL/TM-7948, Oak Ridge National Laboratory (1981).

56. U.S. Nuclear Regulatory Commission, Standard for Protection Against Radiation, US NRC Rules and Regulations, Title 10, Chapter 1, Part 20 (1977).

57. A. E. Profio, Radiation Shielding and Dosimetry, A. Wiley - Interscience Publication, John Wiley & Sons, New York (1979).

58. J. H. Huang and M. E. Sawan, Neutronics Analysis for the MARS Li-Pb Blanket and Shield, J. Nucl. Tech./Fusion 6, No. 2., 883 (1983).

59. H. Attaya, et al., Blanket and Shielding Considerations for Advanced Tokamak Reactor Concepts, UWFDM-562, Fusion Engineernig Program, U. of Wisconsin, Madison, WI (1983).

60. B. Badger, et al., High Wall Loading Compact Tokamak Power Reactor - A Scoping Study, UWFDM-592, Fusion Engineering Program, U. of Wisconsin, Madison, WI (1984).

61. M. Z. Youssef, Status of Methods, Codes and Applications for Sensitivity and Uncertainty Analysis, Proc. of the 6th Topical Mtg. on the Tech. of Fusion Energy, San Francisco, CA, March 3-7, 1985.

62. T. Wu and C. W. Maynard, The Application of Uncertainty Analysis in Conceptual Fusion Reactor Design, A Review of the Theory and Application of Sensitivity and Uncertainty Analysis, Proc. of a Seminar-Workshop, ORNL/RSIC-42, Oak Ridge National Laboratory (1979).

63. D. J. Dudziak, Cross-section Sensitivity and Uncertainty Analysis for Fusion Reactors - A Review, Proc. of the Advisory Group Mtg. on Nuclear Data for Fusion Reactor Technology, IAEA-TECDOC-223, p. 121, IAEA, Vienna (1979).

64. D. Garber, Compiler, ENDF-201/B Summary Documentation, BNL 17541 (ENDF-201), Brookhaven National Laboratory (1978).

65. R. Howerton, et al., The LLL Evaluated-Nuclear-Data Library (ENDL), UCRL-50400, Lawrence Livermore National Laboratory (1978).

66. S. Igarasi, et al., Japanese Evaluated Nuclear Data Library, Version 1, JENDL-1, JAERI 1261, Japan Atomic Energy Institute (1979).

67. J. Story and R. Smith, The 1981 Edition of the United Kingdom Data Library - A Status Summary, informal notes (1981).

68. D. J. Dudziak and P. G. Young, Review of New Development in Fusion Reactor Nucleonics, Proceedings of the Fourth Topical Mtg. on the Technology of Controlled Nuclear Fusion Energy, Conf-801011, Volume I, P.419, King of Prussia, Pennsylvania (1981).

69. D. G. Gardner, Recent Developments in Nuclear Reaction Theories and Calculations, BNL-NCS-51245, P.641, Brookhaven National Laboratory (1980).

70. P. G. Young, E. D. Arthur, and D. G. Madland, Application of Nuclear Model Codes, Proceedings of Intl. Conf. on Nuclear Cross Sections and Technology, Knoxville, TN, 27-29 (Oct. 1979).

71. A. B. Smith, Comments on the $^7Li(n;n',\alpha)t$ Cross Section, Argonne National Laboratory (unpublished).

72. E. Goldberg, et al., Measurements of ^{6}Li and ^{7}Li Neutron-Induced Tritium Production Cross Sections at 15 MeV, UCRL-91930, Lawrence Livermore National Laboratory (1985).

73. D. L. Smith, et al., Cross-Section Measurement for ^{7}Li(n,n't)^{4}He Reaction at 14.74 MeV, ANL/NDM-87, Argonne National Laboratory (1984).

74. M. T. Swinhoe, et al., An Absolute Measurement of ^{7}Li (n,n αt) Reaction Cross Section Between 5 and 14 MeV, J. of Nucl. Sci. and Eng. 89, 261 (1985).

75. H. Liskien, et al., Determination of ^{7}Li(n,n't)^{4}He Cross Sections, Proceedings of the Intl. Conf., 6-10 September 1982, Antwerp, Belgium, Ed. K. H. Bockhoff, D. Reidel Publishing Company, Dordrecht, Holland, p. 349 (1983).

76. K. Shibato, Evaluation of Neutron, Nuclear Data of ^{7}Li for JEND-3, JAERI-M 84-204, Japan Atomic Energy Institute (1984).

77. ENDF/B-V.2 ^{7}Li (Mat. 1397, Mod. 1), evaluated by P. G. Young, Los Alamos National Laboratory (1983).

78. M. A. Abdou, Y. Gohar, and R. Q. Wright, MACK-III, A New Version of MACK: A Program to Calculate Nuclear Response Functions from Data in ENDF/B Format, ANL/FPP-77-5, Argonne National Laboratory (1978).

79. R. E. MacFarlane, Energy Balance of ENDF/B-V, Trans. Am. Nucl. Soc. 33, 681 (1979).

80. R. C. Little and R. E. Seamon, Negative Heating Numbers, Los Alamos National Laboratory (unpublished).

81. E. D. Arthur and P. G. Young, Evaluated Neutron-Induced Cross Sections for ^{54,56}Fe to 40 MeV, LA-8626-MJ (ENDF 304), Los Alamos Scientific Laboratory (1980).

82. E. D. Arthur, Gamma-Ray Production Cross Section Calculations for the Tungsten Evaluation and E. D. Arthur, et al., ^{181,183,184,186}W Evaluations, LA-8757-PR, pp. 3 and 6, Los Alamos National Laboratory (1981).

83. Y. Gohar and M. A. Abdou, MACKLIB-IV: A Library of Nuclear Response Functions Generated with MACK-IV Computer Program from ENDF/B-IV, ANL/FPP/TM-106, Argonne National Laboratory (1978).

84. R. E. MacFarlane and D. G. Foster, Jr., Advanced Nuclear Data for Radiation Damage Calculations, J. of Nucl. Mater. 122&123, 1047 (1984).

Distribution for ANL/FPP/TM-203

Internal:

C. Adams
C. Baker
R. Blomquist
J. Brooks
F. Cafasso
Y. Chang
C. Dennis
D. Ehst
K. Evans
P. Finn
E. Fujita
E. Gelbard
Y. Gohar (10)
L. Greenwood
D. Gruen
C. Johnson
M. Kaminsky
S. Kim
R. Kustom
M. Lineberry
L. LeSage
R. Martin
R. Mattas
B. Misra
A. Smith
D. Smith
C. Till
L. Turner
S. Yang
FPP Files (10)
ANL Contract File
ANL Libraries
TIS Files (5)
ANL Patent Dept.

External:

DOE-TIC, for distribution per UC-20 (107)
Manager, Chicago Operations Office, DOE
University of Chicago Special Committee for the Fusion Program:
S. Baron, Brookhaven National Laboratory
H. K. Forsen, Bechtel National, Inc., San Francisco
J. A. Maniscalco, TRW, Inc., Redondo Beach
G. H. Miley, U. Illinois, Urbana
P. J. Reardon, Brookhaven National Laboratory
P. H. Rutherford, Princeton University
D. Steiner, Rensselaer Polytechnic Institute
K. R. Symon, Synchrotron Radiation Center, Stoughton, WI
K. I. Thomassen, Lawrence Livermore National Laboratory
M. A. Abdou, University of California-Los Angeles
R. G. Alsmiller, Oak Ridge National Laboratory
V. C. Baker, Oak Ridge National Laboratory
K. Barry, The Ralph Parsons Company
S. Berk, DOE
L. A. Berry, Oak Ridge National Laboratory
M. R. Bhat, Brookhaven National Laboratory
B. L. Bishop, Oak Ridge National Laboratory
J. A. Blair, Oak Ridge National Laboratory
A. L. Boch, Oak Ridge National Laboratory
K. H. Bockhoff, Commission of the European Communities
A. Bolon, University of Missouri-Columbia
L. Booth, Los Alamos National Laboratory
R. Brown, Los Alamos National Laboratory
S. Burnett, GA Technologies, Inc.
D. Campbell, Oak Ridge National Laboratory
J. Cannon, Oak Ridge National Laboratory

L. Carter, Hanford Engineering Development Laboratory
G. Casini, C.E.A. Ispra (VA), Italy
C. Clifford, Princeton Plasma Physics Laboratory
R. Conn, University of California-Los Angeles
J. Crocker, EG&G Idaho, Inc.
D. Dudziak, Los Alamos National Laboratory
M. J. Embrechts, Rensselaer Polytechnic Institute
B. Engholm, GA Technologies, Inc.
C. Flanagan, Oak Ridge National Laboratory
K. Furuta, University of Tokyo, Japan
A. Gabriel, Oak Ridge National Laboratory
D. Graumann, GA Technologies, Inc.
H. Gruppelaar, Netherlands Energy Research Foundation
G. Haste, Oak Ridge National Laboratory
R. Howerton, Lawrence Livermore National Laboratory
S. Iwasaki, Lawrence Livermore National Laboratory
D. Jassby, Princeton Plasma Physics Laboratory
R. J. Juzaitis, Los Alamos National Laboratory
S. Kailas, Indiana University
A. C. Klein, Oregon State University
H. Klein, Physikalisch-Technische Bundesanstalt
R. A. Krakowski, Los Alamos National Laboratory
H. Kranse, Max-Planck Institute fur Plasmaphysik, West Germany
A. Knoblock, Max-Planck Institute fur Plasmaphysik, West Germany
J. Kristiak, Slovak Academy of Sciences
L. P. Ku, Princeton Plasma Physics Laboratory
G. Kulcinski, University of Wisconsin-Madison
J. D. Lee, Lawrence Livermore National Laboratory
R. A. Lillie, Oak Ridge National Laboratory
R. J. Livak, Los Alamos National Laboratory
B. G. Logan, Lawrence Livermore National Laboratory
G. Longo, Istituto di Fisica
C. Marinucci, SIN, Villigen, Switzerland
C. Maynard, University of Wisconsin-Madison
H. McCurdy, Oak Ridge National Laboratory
R. Miller, Los Alamos National Laboratory
R. Moir, Lawrence Livermore National Laboratory
D. Montgomery, Massachusetts Institute of Technology
T. Nakamura, Japan Atomic Energy Research Institute
K. Oishi, Shimizu Construction Co., Ltd.
Y. Oka, University of Tokyo, Japan
D. Paul, Electric Power Research Institute
S. Pearlstein, Brookhaven National Laboratory
J. Powell, Brookhaven National Laboratory
R. J. Puigh, Westinghouse Hanford Company
J. Rathke, Grumman Aerospace Corporation
C. Rhilis, CEA
R. P. Rose, Westinghouse Electric Corporation
R. Roussin, Radiation Shielding Information Center, ORNL

P. Sager, GA Technologies, Inc.
E. Salpietro, NET - IPP
R. T. Santoro, Oak Ridge National Laboratory
M. Sawan, University of Wisconsin-Madison
K. R. Schultz, GA Technologies, Inc.
F. Scott, Electric Power Research Institute
J. L. Scott, Oak Ridge National Laboratory
Y. Seki, Japan Atomic Energy Research Institute
T. Shannon, Oak Ridge National Laboratory
Z. Shapiro, Westinghouse Electric Corporation
W. Stacey, Jr., Georgia Institute of Technology
M. Stauber, Grumman Aerospace Corporation
J. D. Stout, Oak Ridge National Laboratory
K. Sumita, Osaka University, Japan
D. W. Swain, Oak Ridge National Laboratory
M. A. Sweeney, Sandia National Laboratories
A. Takahashi, Osaka University
W. L. Thompson, Los Alamos National Laboratory
A. Tsechanski, Ben Gurion University of the Negev
J. Turner, DOE
D. Wattecamps, Commission of the European Communities
G. L. Woodruff, University of Washington-Seattle
V. Zoita, Central Institute of Physics, Bucharest
Librarian, Culham Laboratory, Oxford, England
Library, Centre de Recherches en Physique des Plasma, Lausanne, Switzerland
Library, FOM-Institue voor Plasma-Fysika, The Netherlands
Library Laboratorio Gas Ionizati, Frascatti, Italy
Thermonuclear Library, Japan Atomic Energy Research Institute, Tokyo, Japan